Inclusion Complexes of Dimethyl 2,6-Naphthalenedicarboxylate with α- and β-Cyclodextrins in Aqueous Medium: Thermodynamics and Molecular Mechanics Studies

Marta Cervero and Francisco Mendicuti*

Departamento de Química Física, Universidad de Alcalá, 28871 Alcalá de Henares, Madrid, Spain

Received: September 24, 1999; In Final Form: November 23, 1999

Steady-state fluorescence and molecular mechanics have been used to study the inclusion complexes of dimethyl 2,6-naphthalenedicarboxylate (DMN) with α- and β-cyclodextrins (CDs). Emission spectra of DMN show two bands whose ratio is very sensitive to the medium polarity. From the change of this ratio with CD concentration and temperature, the stoichiometry, the formation constants, and the changes of enthalpy and entropy upon inclusion of complexes formed were obtained. Stoichiometry depends on the host CD used. The estimated formation constants at 25 °C were $(8.2 \pm 0.6) \times 10^5$ M^{-2} for DMN:αCD_2 and 1311 ± 57 M^{-1} for DMN:β$CD. A dependence of the thermodynamic parameters $\Delta H°$ and $\Delta S°$ on the temperature was also found. Both complexes showed a negative $\Delta C_p°$. In addition, DMN seems to be a good probe for estimating microenvironmental polarity. Molecular mechanics calculations were also employed to study the formation of 1:1 and 1:2 complexes of DMN with both α- and βCDs. The study was mainly performed in the presence of water as a solvent. Results seem to explain the stoichiometries for both complexes. Only a small portion of DMN penetrates into the αCD cavity, but it does penetrate almost totally into βCD. This fact makes it possible to stabilize the former 1:1 complex by adding other αCD. The driving forces for both 1:1 and 1:2 inclusion processes are dominated by nonbonded van der Waals host:guest interactions. Nevertheless, head-to-head hydrogen bonding formation between secondary hydroxyl groups of αCDs can also contribute to the stability of the DMN:αCD_2 complex.

Introduction

Cyclodextrins are toruslike macrorings built up from glucopyranose units that are well-known for their ability to form inclusion complexes with small molecules[1−5] and polymer chains.[4,6−13] When guests contain fluorophore groups, fluorescence spectroscopy[14−38] can be a useful tool for obtaining stoichiometry, formation constants, and other thermodynamic parameters upon complexation. Measurements of the enhancement or quenching of the fluorescence emission of guests upon inclusion,[14−24] excimer formation,[25−29] depolarization of the fluoresence,[30] decay of fluorescence,[19,24,31,32] or the relative intensity of some vibronic bands of the emission spectrum are some fluorescence techniques.[33−38] Pyrene is the most well-known molecule that exhibits this last characteristic. Intensity ratios of the named I and III bands can serve as a measure of the polarity of the environment surrounding pyrene.[14,32,33,39]

Complexation processes are reversible in solution and depend mainly on the size, shape, and polarity of the guest molecule relative to the host inner cavity. However, many uncertainties on the driving forces of the inclusion process still remain to be clarified.[1−5] The application of molecular modeling techniques[40,41] can help strengthen experimental results, such as stoichiometry, geometry, and thermodynamics parameters accompanying the complexation process, and they also provide information on the driving forces responsible for such processes.

We have been using molecular mechanics and molecular dynamics to study the inclusion phenomena of small molecules[42−45] and polymers[46−48] with cyclodextrins (CDs). One of these studies was done on the complexation of 2-methyl naphthoate (MN) with α- and βCDs.[42,49] MN emission spectra showed two bands whose ratio of intensities was very sensitive to medium polarity. The analysis of the ratio with the CD concentration revealed the single existence of complexes of stoichiometry 1:1. The estimated formation constants at 25 °C were ∼200 and ∼2000 M^{-1} for αCD and βCD, respectively. Despite the same stoichiometry, the MN inclusion into the αCD cavity was accompanied by a larger negative enthalpy change than the inclusion into the βCD one. Therefore, the MN:αCD complexation was accompanied by a relatively large entropy decrease, whereas the MN:βCD was followed by an entropy increase. Molecular mechanics (MM) studies on both 1:1 complexes[42] in vacuo and in the presence of water showed that the formation of both complexes was favorable with the nonbonded van der Waals interactions as the main contribution to the stabilization. Results indicate that MN totally penetrates into the βCD cavity, but it only slightly penetrates into the cavity of the αCD. This selective ability to insulate MN from the solvent allowed us to explain the signs of ΔS upon binding.

In a similar manner this work reports fluorescence spectroscopy and MM calculations to study the complexation of dimethyl 2,6-naphthalenedicarboxylate (DMN) with α- and βCDs. The stoichiometries, binding constants, $\Delta H°$, and $\Delta S°$ upon complexation were obtained. Experimental results were discussed in comparison with the theoretical MM results of complexation in the presence of water. The effective dielectric constants of CD cavities were estimated and compared with the ones obtained for the MN probe.[49]

Materials and Methods

Materials. Dimethyl 2,6-naphthalenedicarboxylate (DMN) purchased from Aldrich was recrystallized twice from methanol.

* To whom correspondence should be addressed. Phone: 34-91-8854672. Fax: 34-91-8854763. E-mail: francisco.mendicuti@uah.es.

10.1021/jp993418w CCC: $19.00 © 2000 American Chemical Society
Published on Web 01/28/2000

TABLE 1: Bond Lengths, Bond Angles, and Partial Charges in Dimethyl 2,6-Naphthalenedicarboxylate (DMN)

bond	length (Å)	bond	angle (deg)	atom[a]	charges (esu)	atom[a]	charges (esu)
$C^{ar}-C^{ar}$	1.40 ± 0.02	$C^{ar}-C^{ar}-C^{ar}$	120.0 ± 0.6	C(1)	−0.053	C(8)	−0.119
$C^{ar}-C^{*}$	1.47	C(3)−C(2)−C*	117.6	C(2)	−0.097	C(9)	−0.036
C*−O	1.37	C(2)−C*−O	114.3	C(3)	−0.090	C(10)	−0.036
C*═O	1.23	C(2)−C*═O	128.0	C(4)	−0.119	C*	0.343
O−CH_3	1.43	O═C*−O	117.7	C(5)	−0.053	O(═C*)	−0.348
		C*−O−CH_3	116.4	C(6)	−0.097	O(−C*)	−0.279
				C(7)	−0.090	C(−H_3)	−0.062

[a] Charges for hydrogen atoms (not tabulated) produce a neutral molecule.

α-Cyclodextrin and β-cyclodextrin, referred to as αCD and βCD, were also purchased from Aldrich. The βCD was purified before use by recrystallizing it twice from distilled and deionized water (taken from a Milli-Q water system). The αCD was used without further purification. TGA of αCD and βCD reveals 9.8% and 6.0% water content by mass, respectively. Solvents, *n*-alcohols $H(CH_2)_nOH$, from $n = 1$ to 7, ethylene glycol (Aldrich spectrophotometric grade or higher than 98%), and deionized water were checked for impurities by fluorescence before using.

DMN:CD water solutions were prepared by using an aqueous DMN-saturated solution. For this purpose DMN was forced to dissolve in water by keeping the solution in an ultrasonic bath for 1 h and stirring it for an additional 48 h. The solution was then filtered twice through 0.45 μm diameter size cellulose filters (Millipore), giving a saturated DMN water solution ($\sim 10^{-6}$ M). DMN:CD water solutions were prepared by weight in their own quartz cuvettes using the DMN-saturated solution as a solvent. The cuvettes were then perfectly sealed with Teflon stoppers. All solutions were stirred in their own cuvettes for 48 h. Concentrations of αCD and βCD ranged from 0 to 1.269×10^{-2} M and from 0 to 1.183×10^{-2} M, respectively. The DMN concentration was held constant in all experiments.

Fluorescence Measurements. Steady-state fluorescence measurements were performed by using an SLM 8100 AMINCO spectrofluorometer equipped with a cooled photomultiplier and a double monochromator in the excitation path. Slit widths were 8 nm for excitation and emission. The cell housing (1 cm path cells) was controlled at the temperature of interest by using a bath (Techne RB-5) equipped with a power head (Techne TE-8A). Polarizers were set for the magic angle conditions. Emission spectra were obtained at 294 nm as excitation wavelength. Fluorescence measurements of DMN:CD water solutions were performed in the range of temperatures from 5 to 45 °C at 10 °C intervals.

Computational Details. The calculations were performed with Sybyl 6.4[50] using the Tripos force field.[51] The total potential energy of a system was obtained as the sum of six contributions: bond stretching, angle bending, torsion, van der Waals, electrostatics, and out-of-plane. A relative permittivity $\epsilon = 3.5$ and a function of the distance, $\epsilon = \epsilon_0 r$ (where $\epsilon_0 = 1$ and r is the interatomic distance), were used for electrostatics interactions in vacuo and in the presence of water, respectively. Guest (DMN) geometry and charges, obtained by MOPAC,[52] are collected in Table 1. Geometry and charges of CDs and water molecules, also obtained by MOPAC, were used previously.[42−48] Extended nonbonded cutoff distances were set at 8 Å for van der Waals and electrostatics interactions. Minimization of the potential energy of the system was performed by the simplex algorithm, and the conjugate gradient was used as a termination method.[53,54] The termination gradients were 0.2 and 3.0 for the calculations performed in vacuo and in water, respectively. Solvation was achieved by using the Molecular Silverware[55] algorithm (MS). PBC conditions were employed using a cubic box with side of 31.62 Å (32.38 Å) for 1:1 complexes and 31.83 Å (32.56 Å) for 1:2 ones with αCD (βCD).

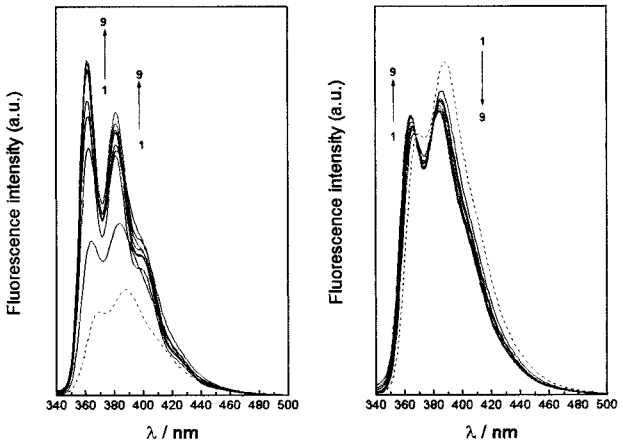

Figure 1. Uncorrected emission spectra of DMN (- - -) and DMN:CD (α- or βCD) aerated aqueous solutions at different CD concentrations and [DMN] constant at 25 °C upon excitation at $\lambda_{exc} = 294$ nm: (left) [αCD] = 0 (1), 0.000 85 M (2), 0.001 30 M (3), 0.002 15 M (4), 0.003 97 M (5), 0.006 62 M (6), 0.009 35 M (7), 0.010 57 M (8), and 0.012 69 M (9); (right) [βCD] = 0 (1), 0.000 47 M (2), 0.000 949 M (3), 0.001 18 M (4), 0.001 42 M (5), 0.002 84 M (6), 0.005 68 M (7), 0.008 52 M (8), and 0.011 83 M (9).

The binding energy $E_{binding}$(guest:host), which is associated with the enthalpy change, between the guest and the host for a 1:1 complex, either for the nonsolvated structures or for the solvated ones, was obtained as the difference between the potential energy of the guest:host system and the sum of the potential energies of the isolated guest and host in the same conformation as

$$E_{binding}(\text{guest:host}) = E_{guest:host} - (E_{isolated\ host} + E_{isolated\ guest})$$

In a similar way, for the study of 1:2 complexes two different binding energies named $E_{binding}$(host1:guest−host2) and $E_{binding}$(guest−(host1+host2)) were also calculated. Any nonbonded A−B interaction (or any of the contributions) between two components (A) and (B) of a system (A + B) can be obtained as the difference of the total potential energy of the whole system (A + B) and the sum of the potential energies of isolated A and B in the same conformation. The strain energy of CDs was obtained as the sum of torsional, stretching, and bending energies. For evaluating the number of potential hydrogen bonds (HB), a HB is assumed when the distance between the hydrogen (H), bonded to a donor (D) and the acceptor (A), is in the range 0.8−2.8 Å and the angle D−H−A is >120°.

Results and Discussion

Emission Spectra. Figure 1 depicts the uncorrected emission spectra of DMN in water and in aqueous αCD and βCD at different CD concentrations at 25 °C. The main feature of both groups of spectra is the presence of two main bands centered

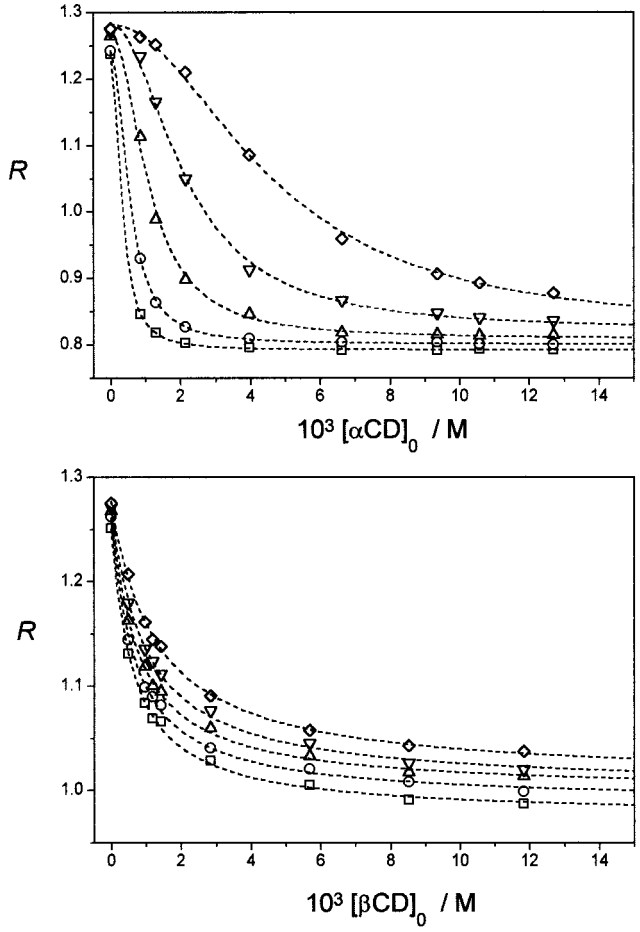

Figure 2. Ratios R of band intensities at the maxima (381−385 and 361−365 nm) for DMN vs [αCD] (top) and [βCD] (bottom) at different temperatures: 5 °C (□), 15 °C (○), 25 °C (△), 35 °C (▽), and 45 °C (◇). Dashed lines were obtained by adjusting the experimental data to the proper stoichiometry by using eq 5.

around 361−365 nm and 381−385 nm, which also appear in the emission spectrum of the free DMN water solution. An increase in the fluorescence intensity as the CD concentration increases is observed for the DMN:αCD system; however, the fluorescence intensity seems to be almost constant for the DMN:βCD one. A small shift to the blue of the emission spectra and especially a change in the relative intensity of the two bands with CD concentration and temperature are also observed for both sets of experiments. An isosbestic point around 368 nm for the DMN:βCD system indicates the presence of an equilibrium; this fact is not inferred from the emission spectra of DMN:αCD solutions. A common feature of both series of spectra is that at each temperature, as αCD or βCD concentrations increase, the ratio R of intensities measured at the maximum of the low (381−385 nm) and the high (361−365 nm) energy bands respectively decreases. However, the shape and amount of this decrease depend on the CD used. This change in R is associated with the change in the polarity of the microenvironment surrounding the DMN probe during complexation. The lower value of R should suggest that more DMN guest molecules are complexed; that is, more DMN molecules are located inside the more apolar medium. Figure 2 shows the effect of increasing concentrations of αCD and βCD on the ratio R at different temperatures. The shape of these curves and the value of the CD concentration at which curves level off for both systems suggest different stoichiometry complexes and different association constants. The value of R at high CD concentrations at each temperature, when all DMN is complexed, R_∞, is different for both αCD and βCD complexes, and it also differs from the one obtained for free DMN in water, R_0. R_∞ should give information about the medium polarity of the inner CD cavity.

Considering a 1:n DMN:CD stoichiometry, the complexation of DMN in the CD cavity follows the equilibrium

$$\mathrm{DMN} + n\mathrm{CD} = \mathrm{DMN{:}CD}_n \tag{1}$$

and the association constant K can be expressed as

$$K = \frac{[\mathrm{DMN{:}CD}_n]}{[\mathrm{DMN}][\mathrm{CD}]^n} \tag{2}$$

Substituting the mass balance expressions for DMN and CD and assuming that the initial analytical concentration of CD is $[\mathrm{CD}]_0 \gg [\mathrm{DMN{:}CD}_n] \gg [\mathrm{DMN{:}CD}_{n-1}]$, etc., for equilibrium 1 and that R is the weighted average from the DMN-complexed fraction f (=$[\mathrm{DMN{:}CD}_n]/[\mathrm{DMN}]_0$) evaluated as[35]

$$f = \frac{R_0 - R}{R_0 - R_\infty} \tag{3}$$

where R_0, R_∞, and R are the defined ratio for DMN free, in the complex, and measured at a given CD concentration, respectively, result in

$$\frac{1}{R_0 - R} = \frac{1}{R_0 - R_\infty} + \frac{1}{K(R_0 - R_\infty)[\mathrm{CD}]_0^n} \tag{4}$$

A named double-reciprocal plot of $1/(R_0 - R)$ vs $[\mathrm{CD}]_0^{-n}$ should give a straight line. Dividing the intercept by the slope gives the stability constant for the 1:n stoichiometry of the $\mathrm{DMN{:}CD}_n$ complex. Figure 3 depicts double reciprocal plots at different temperatures assuming different 1:1 or 1:2 stoichiometries for both complexation processes with α- and βCD. Linear relationships in the range of the CD concentrations checked are indicative of the 1:2 and 1:1 DMN:host complex formation with α- and βCD, respectively. Any attempt to adjust the experimental data to stoichiometries other than the real ones resulted in an upward (Figure 3a) or downward (Figure 3d) concave curvature of these plots. Even at very low αCD concentrations there is no real evidence of 1:1 DMN:αCD complex formation.

However, a double-reciprocal plot weighs more, $1/(R_0 - R)$ values of the points having the lowest CD concentrations because the slope is very sensitive to these values. A nonlinear regression analysis is sometimes better for analyzing the experimental results.[56] This analysis was also used by fitting the experimental data to the equation

$$R = \frac{R_0 + R_\infty K[\mathrm{CD}]_0^n}{1 + K[\mathrm{CD}]_0^n} \tag{5}$$

derived simply from eq 4.

Table 2 collects the estimated binding constants for the 1:2 and 1:1 DMN:host complexes with α- and βCD respectively at different temperatures by using this method. This table also summarizes the values of parameters R_0 and R_∞. The curves depicted in Figure 2 were obtained by adjusting experimental data to eq 5. Different values of R_0 with temperature simply denote the influence of the temperature on both bands for isolated DMN in water.

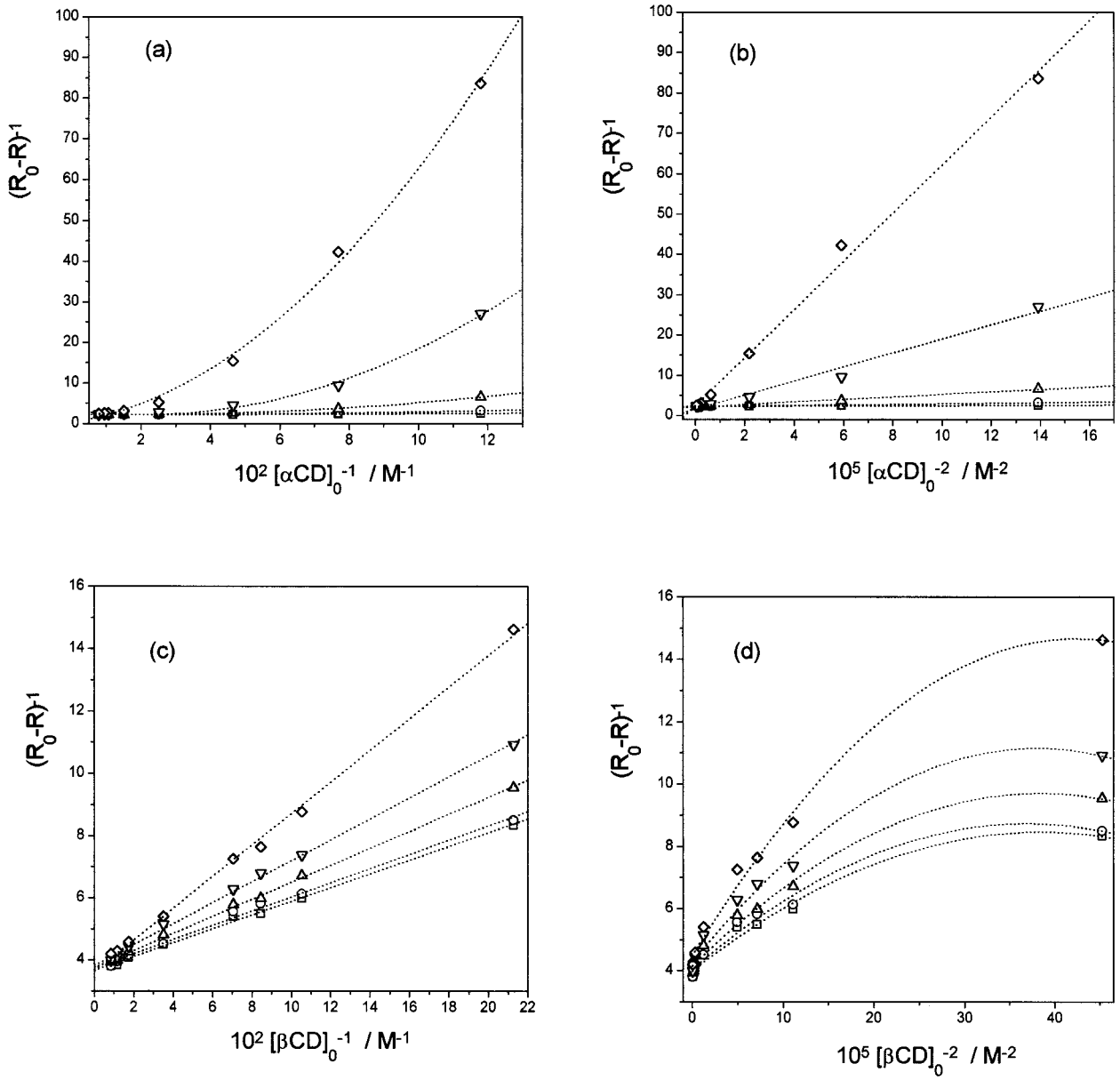

Figure 3. Double-reciprocal plots $(R_0 - R)^{-1}$ vs $[CD]^{-1}$ and $[CD]^{-2}$ for DMN complexed with αCD (a, b) and *β*CD (c, d) at different temperatures: 5 °C (□), 15 °C (○), 25 °C (△), 35 °C (▽), and 45 °C (◇).

TABLE 2: Equilibrium Constants *K*, R_0, and R_∞ and Their Absolute Errors for DMN:αCD$_2$ and DMN:*β*CD at Five Temperatures, Determined by Using Nonlinear Regression Fits from Eq 5

	DMN:αCD$_2$			DMN:*β*CD		
T (°C)	$K \times 10^{-3}$ (M^{-2})	R_0	R_∞	*K* (M^{-1})	R_0	R_∞
5	9901 ±350	1.237 ± 0.002	0.792 ± 0.001	1576 ± 76	1.250 ± 0.003	0.975 ± 0.001
15	3383 ± 58	1.242 ± 0.002	0.801 ± 0.001	1481 ± 83	1.261 ± 0.004	0.989 ± 0.001
25	819 ± 59	1.268 ± 0.001	0.808 ± 0.004	1311 ± 57	1.267 ± 0.003	0.999 ± 0.004
35	215 ± 19	1.283 ± 0.008	0.821 ± 0.006	1027 ± 57	1.269 ± 0.004	1.002 ± 0.003
45	46 ± 4	1.282 ± 0.005	0.817 ± 0.009	789 ± 28	1.277 ± 0.002	1.010 ± 0.002

Because of the dependence on the ratio *R* with medium polarity, the values of R_∞ were used to evaluate the effective polarity of the medium surrounding DMN when complexed with CDs. As previously,[49] emission spectra for DMN in different polarity media, by using several solvents such as methanol/water and ethanol/water mixtures and the series of *n*-alcohols from methanol to heptanol, were obtained. Emission spectra of all solutions are very similar to the ones depicted in Figure 1 for DMN:CD solutions, showing two main bands. The dependence of the ratio *R* with ϵ at 25 °C is depicted in Figure 4, and the equation that best describes the plot is $R = 0.79036 + (2.94 \times 10^{-3})\epsilon + (4.21 \times 10^{-5})\epsilon^2$. From the data of R_∞ at 25 °C collected in Table 2, the estimated dielectric constants of the media surrounding DMN when totally complexed with α- and *β*CD are ∼6 and ∼45, respectively. These values are in agreement with those reported by Street et al.[34] and us,[49] by using pyrene-3-carboxaldehyde and 2-methyl naphthoate (MN) probes, respectively.

The values of *K* for DMN:αCD$_2$ and DMN:*β*CD complexes, which are collected in Table 2, can change from (9901 ± 350) × 10^3 M^{-2} and 1576 ± 76 M^{-1} at 5 °C to (46 ± 4) × 10^3 M^{-2} and 789 ± 28 M^{-1} at 45 °C, respectively. These values indicate

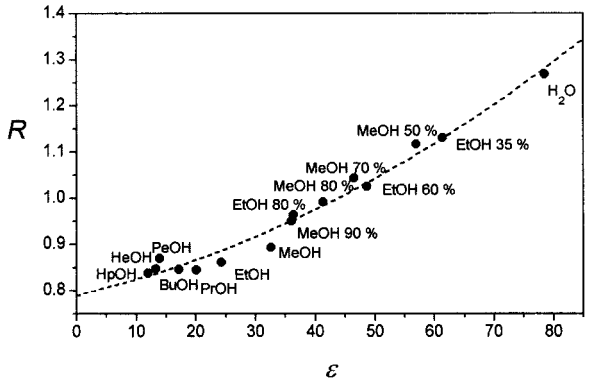

Figure 4. Calibration plot of R vs the solvent dielectric constant ϵ obtained from the emission spectra for dilute solutions of DMN in different solvents at 25 °C. Solvents are methanol−water and ethanol−water mixtures (% vol) and a series of *n*-alcohols (MeOH, EtOH, PrOH, BuOH, PeOH, HeOH, and HpOH).

that approximately 99% of DMN is complexed with two αCDs while approximately 86% of DMN is incorporated into the βCD cavity at a temperature of 5 °C when $[CD]_0 \approx 4.0 \times 10^{-3}$ M. However, only about 42% and 76% of DMN is complexed with α- and βCD, respectively, at 45 °C and at the same CD concentration. Several authors,[17,28,30−32,57−62] including us,[49] have reported a variety of values for binding constants of 1:1 complexes of naphthalene derivative compounds with βCD and a few others with αCD.[22,31,59,62−64] Catena et al.[30] demonstrate the presence of 1:1 and 1:2 complexes of some anilinonaphthalenesulfonates and βCD. Köhler[62] reported the formation of 1:1 and 1:2 complexes of 2-naphthol with αCD. K_1 and K_2 constants were estimated to be approximately 250 and 35 M^{-1}, respectively, at 25 °C. Hamai[63,64] also found the coexistence of 1:1 and 1:2 stoichiometry complexes of some naphthalene halogenated guest molecules with αCD at the same temperature. The values of K_1 and K_2 obtained were 560 and 530 M^{-1} for the 6-bromo-2-naphthol guest[63] and 292 and 246 M^{-1} for the 2-chloronaphthalene one.[64]

K_1 and K_2 constants calculated by us according to a stepwise complexation process (not tabulated here) reveals that $K_2 \gg K_1$ at any temperature, suggesting that 1:1 DMN:αCD is very unstable and that once the 1:1 complex is formed, it immediately complexes with another αCD. In our previous study of the complexation of 2-methyl naphthoate (MN) containing a single $-COOCH_3$ group instead of two as DMN, only 1:1 complexes with both α- and βCDs were obtained.[49]

The top of Figure 5 depicts the van't Hoff plot of $R \ln K$ vs T^{-1} for the complexes studied. A slightly nonlinear behavior reveals the dependence of $\Delta H°$ and $\Delta S°$ with temperature, pointing out a complexation process with $\Delta C_p° \neq 0$. Then the dependence on temperature for $\Delta H°$ and $\Delta S°$ can be expressed by

$$\Delta H°(T) = \Delta H° + \Delta C_p°(T - 298.15) \quad (6)$$

$$\Delta S°(T) = \Delta S° + \Delta C_p° \ln(T/298.15) \quad (7)$$

assuming the independence of $\Delta C_p°$ with temperature and taking 298.15 K as the reference temperature. The thermodynamics parameters $\Delta H°$, $\Delta S°$, and $\Delta C_p°$ at 298.15 K are related to $R \ln K$ through the van't Hoff equation,

$$R \ln K = -[\Delta H° + \Delta C_p°(T - 298.15)]/T + [\Delta S° + \Delta C_p° \ln(T/298.15)] \quad (8)$$

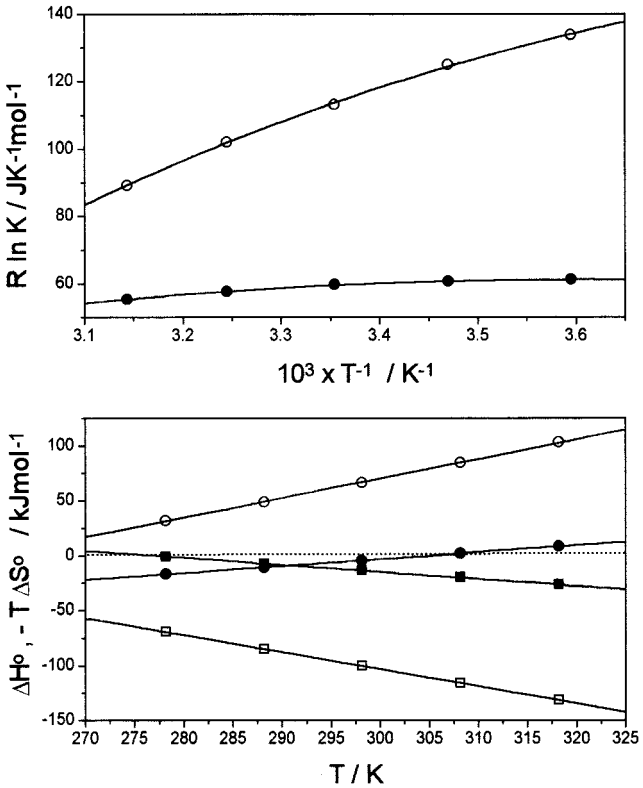

Figure 5. (Top) van't Hoff plots of $R \ln K$ vs T^{-1} for the formation of DMN:αCD_2 (○) and MN:βCD (●) complexes. Curves were obtained by fitting the data to eq 8. (Bottom) Variation of ΔH (squares) and $-T\Delta S$ (circles) for DMN:αCD_2 (open symbols) and MN:βCD (solid symbols) with temperature.

TABLE 3: Values of the Enthalpy ($\Delta H°$), Entropy ($\Delta S°$), and the Heat Capacity ($\Delta C_p°$) Changes of the Complexation Processes of DMN:αCD_2 and DMN:βCD at 298.15 K

host	$\Delta H°$ (kJ mol^{-1})	$\Delta S°$ (J K^{-1} mol^{-1})	$\Delta C_p°$ (J K^{-1} mol^{-1})
αCD	-100.4 ± 1.6	-223.1 ± 5.2	-1553 ± 262
βCD	-13.4 ± 0.3	$+14.7 \pm 1.2$	-643 ± 59

which is simplified by the known linear relation when $\Delta C_p° = 0$. The $\Delta H°$ and $\Delta S°$ at 298.15 K, calculated by fitting the experimental data depicted on top of Figure 5 to eq 8 by using a nonlinear regression analysis,[56] are listed in Table 3 for both the α- and βCD complexes. As usual, both complexes show negative enthalpy changes. The $\Delta H°$ for the formation of the 1:1 DMN:βCD complex (-13.4 kJ mol^{-1}) is similar in magnitude to the values obtained for 1:1 complexes of βCD with naphthalene, 2-acethylnaphthalene,[22] 2-methoxynaphthalene,[28] some anilinonaphthalenesulfonates,[30] 2-methyl naphthoate (MN),[49] or other naphthalene-containing guests.[57−61] Something similar occurs with $\Delta S°$ ($+14.7$ J K^{-1} mol^{-1}) for DMN:βCD. Reported entropy $\Delta S°$ values for naphthalene and naphthalene derivative complexes with CDs can either be positive or negative and tend to vary over a range of the same order of magnitude as the one obtained for DMN:βCD.[22,28,30,43,49,57−61] The $\Delta H°$ (-100.4 kJ mol^{-1}) and $\Delta S°$ (-223.1 J K^{-1} mol^{-1}) values for the formation of the DMN:αCD_2 complex are obviously much higher than that for the MN:αCD complex[49] and other naphthalene derivatives.[31,32,59] However, they are more like the ones found for other supramolecular species with a stoichiometry larger than 1:1, such as those from the association of some 1:1 complexes into homo- or heterodimers.[65]

The bottom of Figure 5 depicts the dependence of $\Delta H°$ and $\Delta S°$ on T in the range of temperature of our measurements.

These results call for some remarks. The DMN:αCD$_2$ complex is enthalpy-favored and entropy-disfavored, showing both $\Delta H°$ and $\Delta S°$ negative in the whole range of temperatures studied. However, the 1:1 DMN:βCD complex shows $\Delta S° < 0$ at temperatures higher than approximately 32 °C and $\Delta S° > 0$ at $T < 32$ °C. Something similar occurs with $\Delta H°$, which is usually negative, but at temperatures smaller than approximately 4 °C, $\Delta H° > 0$. As a consequence of this dependence on T, at about $T > 18$ °C the complexation process is enthalpy-governed, while at $T < 18$ °C the process is entropy-driven. This pattern is usually found for association processes in biological systems.[69] Heat capacities $\Delta C_p°$ for both complexes are strongly negative and are approximately twice as large for the compound containing 1:2 stoichiometry. Negative $\Delta C_p°$ values are found for the transfer of apolar guests from water to nonaqueous hydrophobic environments such as CDs. A larger negative value for the 1:2 DMN:αCD complex than for the 1:1 DMN:βCD one could account for the fact that the DMN guest should be more efficiently buried in the higher hydrophobic cavity formed by the two αCD hosts.[66−68]

The $\Delta S° = +14.7$ J K^{-1} mol^{-1} for DMN:βCD at 25 °C is similar to the values of $\Delta S°$ obtained for 1:1 complexes of MN with β-[49] or γCDs.[43] MN is a relatively small guest that can penetrate totally into β- or γCD cavities. This result contrasts with the one obtained for the complexation of large guests into relatively smaller cavities, which are entropically unfavored. Examples are MN into αCD[49] and 9-methyl anthracenoate and 1-methyl pyrenoate into βCD.[45] When part of the guest is outside the cavity in contact with solvent, the positive contribution to ΔS from loss of solvation guest molecules is minimized, and its loss in rotational and translational degrees is the reason for $\Delta S < 0$. Here, DMN should be well shielded from the solvent molecules in the 1:2 DMN:αCD$_2$ complex, ensuring that the strong $\Delta S < 0$ is due to the loss of degrees of rotational and translational freedom during the process. Nevertheless, MM calculations in the next section should confirm these conclusions.

Molecular Mechanics Calculations. As in other studies,[42,44−48] the initial structure of the α- and βCD were in the nondistorted form: (a) the torsional angles ϕ and ψ, defined by C(4)−C(1)−O−C(4′) and C(1)−O−C(4′)−C(1′), respectively, were fixed at 0° and −3°; (b) all glycosidic oxygen atoms O(4′) were placed in the same plane; (c) the bond angles at the bridging oxygen atom, τ, were at 130.3° and 121.7° for α- and βCD, respectively; (d) the χ dihedral angles were initially in the trans conformation. The ester groups for the DMN guest molecule were in the same plane of the naphthalene ring and the dipole moments oriented in opposite directions as depicted in Figure 6.

For the 1:1 inclusion process the center of mass of the glycosidic oxygen atoms of the CD molecule (denoted by *O* in the top portion of Figure 6) was located at the origin of the Cartesian coordinate system. The *y* axis of this coordinate system refers to the *n*-fold rotation CD axis (*n* is the number of glucopyranose units of each CD). The *z* axis passes through one of the *n* glycosidic oxygens, and these oxygen atoms define the *xz* plane. The host−guest distance was taken by the *OO′* distance along the *y* coordinate, where *O′* represents the center of the DMN guest naphthalene ring. The inclusion angle θ was measured between *yz* and the guest naphthalene ring planes. The orientation of the C(9)−C(10) axis of the naphthalene ring relative to the *n*-fold rotation CD axis was measured by the ϵ angle defined by *OO′* and C(9) of the naphthalene group. For the 1:1 complexation process, depicted by the top portion of Figure 6, the guest molecule was incrementally moved in small steps along the *y* axis and forced to pass through the CD cavity.

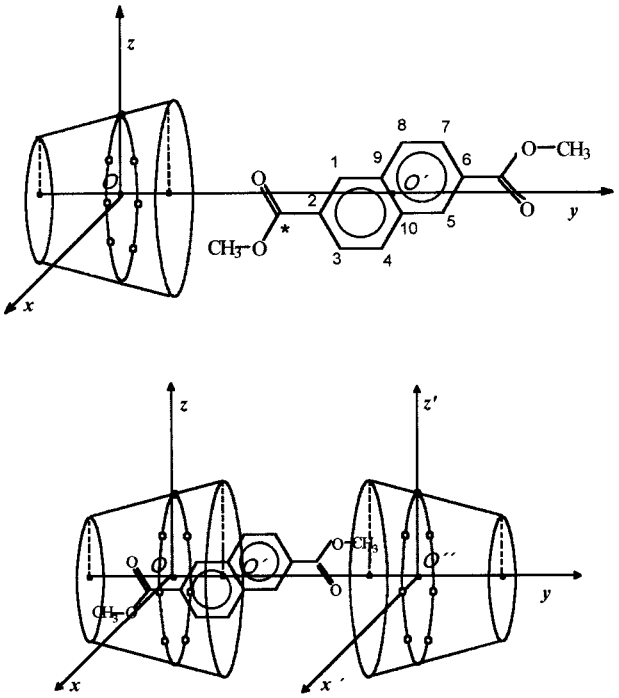

Figure 6. Coordinate systems used to define the processes of 1:1 (a) and 1:2 DMN:host complexation.

In a similar manner, a 1:2 complexation process was simulated by the head-to-head incorporation to the previously formed 1:1 guest:host complex of another CD, according to a scheme that is also depicted at the bottom of Figure 6. Then the structure of minima binding energy of each of the 1:1 complexes was placed with the center of mass of glycosidic oxygen atoms *O* of the CD (host1) at the origin of the coordinate system defined in the previous paragraph, and the center of mass of the glycosidic oxygen atoms *O″* of the other CD (host2) at 15 Å on the positive side of the *y* axis. Then host2 was approached step by step toward the origin *O*. Now *OO″* defines the distance between the CDs along the *y* axis. The association angle θ' is now measured by the angle *O*(*4*)−*O′*−*O″*−*O*(*4″*) where *O*(*4*), *O*(*4″*) are glycosidic oxygens of the host1 and host2 CDs. θ and θ' angles slightly change upon association from the initial θ_{min} and 0° values, respectively.

Initially, the most favorable θ and ϵ angles upon approaching of the DMN to the CD were estimated in vacuo. For this purpose, $E_{binding}$(guest:host) for all optimized structures were obtained by scanning the inclusion angle θ from 0 to 60° at 5° intervals and the *OO′* distance along the *y* coordinate from 16 to −4 Å at 2 Å intervals for three different values of the ϵ angle 50, 90, and 130°. Initial inspection of these results shows that the smallest binding energies for DMN approaching either α- or βCDs are obtained for ϵ around 50−60°. In a second step, similar calculations were performed by initially fixing ϵ at 55° and ranging both *OO′* distance and θ as in the previous calculation. Critical analysis of the three-dimensional plots, obtained from the minimized structures, shows the possible trajectory of the smallest binding energies for the ϵ and θ pairs of ∼60° and ∼15° for the DMN to αCD approach and ∼70° and ∼16° for the DMN to βCD approach. These angles were used initially for simulation of 1:1 inclusion processes.

The remaining calculations were performed in the presence of water. Each structure generated upon the guest to host approach was solvated by using the MS algorithm[55] and then the energy was minimized, as was described previously.[42−45]

1:1 DMN:CD Complexes. Figure 7 depicts the variation of

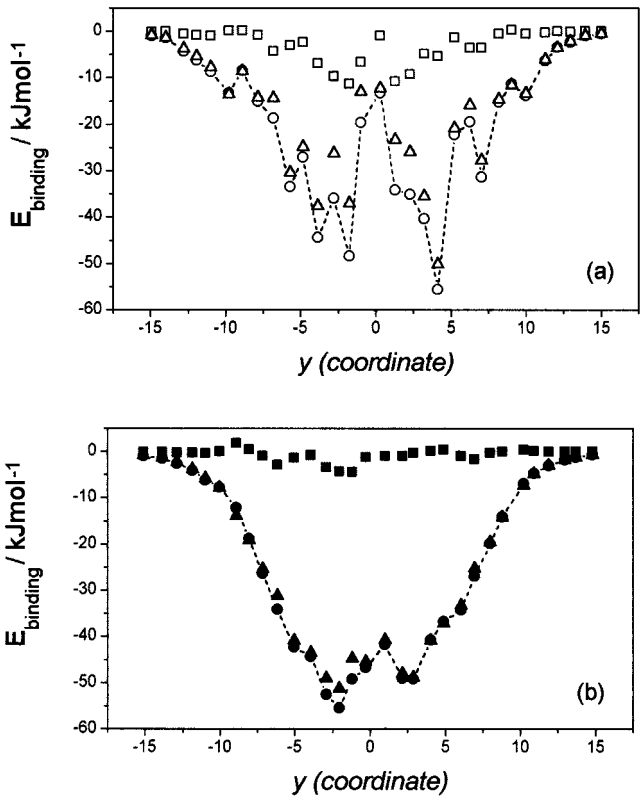

Figure 7. van der Waals (triangles) and electrostatic (squares) contributions to $E_{binding}$ (circles) as a function of y coordinate (Å) for 1:1 DMN:host complexations for host (a) αCD and (b) βCD.

$E_{binding}$, van der Waals, and electrostatic contributions for DMN:αCD and DMN:βCD complexes obtained by scanning y from 15 to −15 Å at 0.5 Å intervals for the trajectories of ϵ and θ initially located at the fixed values described previously. Structures of minima values of binding energies are reached for $y = +4.1$ Å and −2.1 Å and (ϵ_{min}, θ_{min}) angle pairs of (70.1°, 9.8°) and (62.7°, 12.7°) for both DMN:αCD and DMN:βCD complexes, respectively. This indicates that the DMN guest penetrates almost totally into the βCD cavity but just a small portion of the guest penetrates into the αCD one. The top of Figure 8 depicts the structure of minima binding energy for the DMN:βCD (1:1) complex. The fact that most of the guest molecule is shielded by the βCD host could corroborate that the disruption of the water shell around the DMN upon complexation could be responsible for the increase in entropy, since the loss of translational and rotational freedom degrees of the DMN guest should decrease it. Values of $E_{binding}$ and contributions at the minimum (and at ∞ guest−host distance) are collected in Table 4. They are very similar, around −55.5 kJ mol^{-1}, for both structures. van der Waals and electrostatics nonbonded contributions are also very similar. Approximately 90% of $E_{binding}$ at the minimum is due to van der Waals host−guest interactions. As collected in Table 4, the DMN:αCD complexation process is accompanied by an increase of total potential energy, which is mainly due to the increase in αCD macroring strain and electrostatics interactions upon complexation. However, the DMN:βCD complexation is followed by a slight decrease in potential energy. In this case, the electrostatic contributions seem to decrease slightly upon complexation. Figure 9 shows the variation of total potential energy of the CDs, as well as several contributions upon complexation. Complexation produces an increase in the energy of αCDs that is smaller for βCDs. Torsional, bending, and stretching terms contribute to most of this increase.

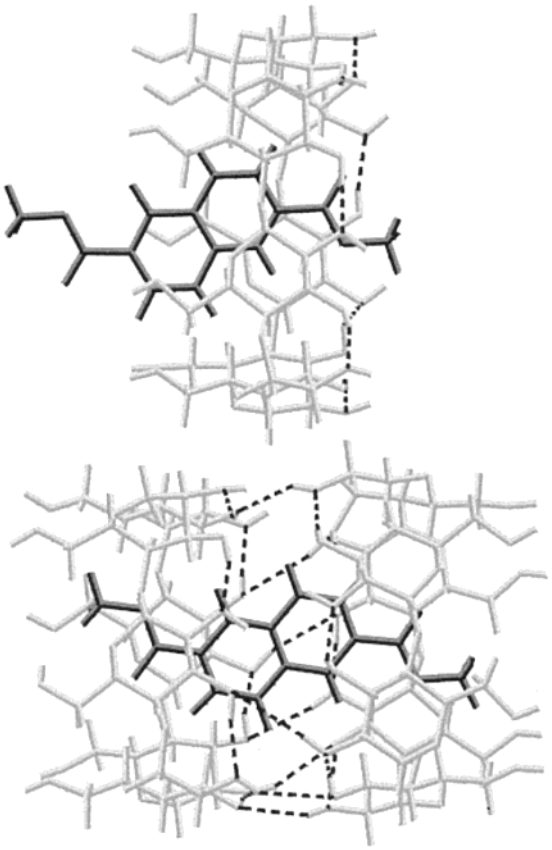

Figure 8. Structures of minimum binding energy for (top) 1:1 DMN:βCD and (bottom) 1:2 DMN:αCD$_2$ complexes. Water molecules were removed.

TABLE 4: $E_{Binding}$ and Selected Components (kJ mol^{-1}) at the Minimum Energy (Subscript "min") at the Largest Separation of the Two Components (Subscript "∞") for DMN:Host 1:1 Complexes in the Presence of Water

	host			
energy (kJ mol^{-1})	αCD$_{min}$	αCD$_{\infty}$	βCD$_{min}$	βCD$_{\infty}$
$E_{binding}$	−55.5	−0.5	−55.5	−0.7
electrostatic part	−5.4	0.0	−4.2	0.0
van der Waals part	−50.2	−0.5	−51.3	−0.7
E_{tot} for DMN:host	661.2	588.9	659.8	672.5
electrostatic part	199.6	179.9	220.0	239.1
van der Waals part	34.7	45.2	16.3	44.2
E_{tot} for host	629.7	526.1	640.2	602.6
electrostatic part	185.4	161.1	205.2	220.8
van der Waals part	66.9	25.2	47.5	25.7
stretching + bending + torsion	377.4	339.9	387.5	356.2
E_{tot} for DMN	87.0	63.3	75.1	70.6
electrostatic part	19.5	18.9	19.1	18.3
van der Waals part	17.9	20.5	20.0	19.3
stretching + bending + torsion	48.2	23.7	34.5	32.6

1:2 DMN:CD Complexes. Figure 10 depicts the variation of the binding energy between the DMN guest and two CD hosts (host1 + host2), named $E_{binding}$(DMN−(host1+host2)), during the approach of a new CD (host2) to the 1:1 complexes (DMN:host1) with minima $E_{binding}$ obtained previously, according to the scheme depicted at the bottom of Figure 6. Figure 10 also includes van der Waals and electrostatics contributions. Minima energy structures are reached at y coordinates for the centers of mass O'' and O' of +8.1 and +4.2 Å for the DMN:αCD$_2$ complex and of +6.5 and −1.4 Å for the DMN:βCD$_2$ one. $E_{binding}$(DMN−(host1+host2)) for these structures were −93.0 and −75.3 kJ mol^{-1} with van der Waals as the most important contribution for both processes. A DMN:host$_2$ formation seems

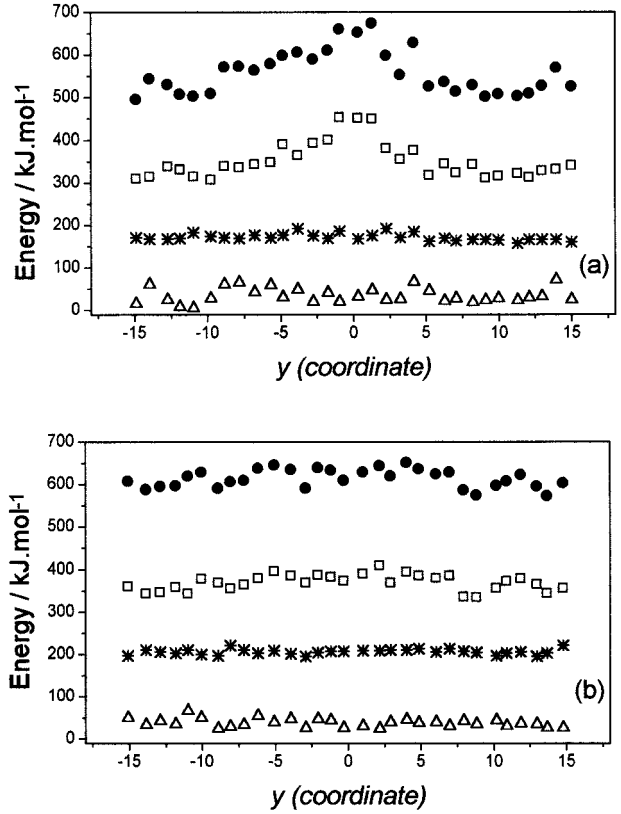

Figure 9. Different contributions to the total potential energy of the solvated conformations as a function of *y* coordinate for (a) αCD and (b) *β*CD hosts. The energies are (●) total, (△) van der Waals, (∗) electrostatic, and (□) strain.

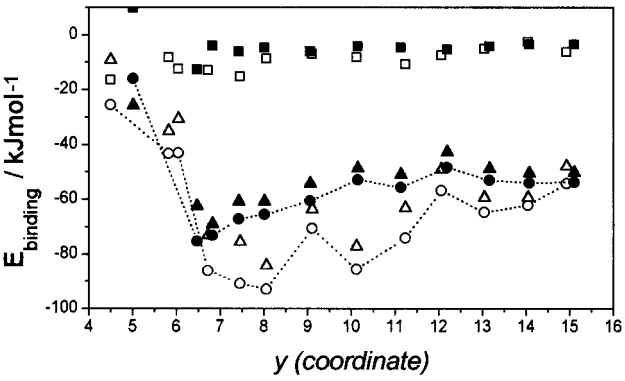

Figure 10. van der Waals (triangles) and electrostatics (squares) contributions to $E_{binding}$(DMN−(host1+host2)) (circles) as a function of the distance between CD hosts along the *y* coordinate for (open symbols) αCD and (solid symbols) *β*CD hosts.

to be more favored when the CD hosts are αCDs than when they are *β*CDs. Table 5 also collects binding energies between the 1:1 complex and the new CD (host2), as well as between both CDs for such structures. These energies are named $E_{binding}$(DMN:host1−host2) and $E_{binding}$(host1−host2), respectively, in Table 5. $E_{binding}$(DMN:host1−host2) also shows the stabilization of the DMN:αCD upon the approach of the second αCD (−71.1 kJ mol^{-1}) contributing both negative van der Waals and electrostatics interactions to such stabilization. However, according to data collected in Table 5, the approach of a second *β*CD to the 1:1 DMN:*β*CD complex is accompanied by an unfavorable positive binding energy (+2.2 kJ mol^{-1}), which comes from the balance of a strong attractive electrostatic interaction, mainly between *β*CDs, and an even stronger repulsive van der Waals interaction between them, which

TABLE 5: $E_{Binding}$ Energies and Selected Components (kJ mol^{-1}) at the Minimum Energy (Subscript "min") and at the Largest Separation of the Two Components (Subscript "∞") for host2 Approaching to DMN:host1 1:1 Complex To Form DMN:(host)$_2$ Complexes in the Presence of Water

	host			
energy (kJ mol^{-1})	αCD_{min}	αCD_{∞}	βCD_{min}	βCD_{∞}
$E_{binding}$(DMN−(host1+host2))	−93.0	−54.4	−75.3	−53.9
electrostatic part	−8.8	−6.4	−12.8	−3.5
van der Waals part	−84.2	48.0	−62.5	−50.5
$E_{binding}$(DMN:host1−host2)	−71.1	−7.7	+2.2	−0.1
electrostatic part	−10.8	0.1	−49.3	−0.1
van der Waals part	−60.3	−7.8	+51.5	−0.1
$E_{binding}$(host1−host2)	−25.6	−0.2	+30.9	−0.1
electrostatic part	−7.7	0.2	−42.4	−0.0
van der Waals part	−17.9	0.0	+73.3	−0.1
E_{tot} for DMN:(host)$_2$ complex	1108.7	1104.8	2364.9	1200.5
electrostatic part	370.3	374.4	483.3	414.6
van der Waals part	−3.8	20.5	387.6	25.8
stretching + bending + torsion	739.5	708.5	1493.4	759.4

considerably increases at *β*CD distances smaller than approximately 8 Å. $E_{binding}$(host1−host2) also shows this fact. The large increase in total energy E_{tot} of hypothetical DMN:βCD_2 upon complexation, and especially the large strain energy, also indicates that this complex is not very favored. However, all results collected in the first two columns infer that the DMN:αCD_2 complex formation is favored. Part of this stabilization must also arise from the presence of intermolecular hydrogen bonds (HB) between αCDs, which are favored when CDs are not very much distorted. This is the case; during the αCD to DMN:αCD approach, αCDs do not significantly distort. According to the criteria of HB formation, the structure of minimum $E_{binding}$(DMN−(host1+host2)) depicted at the bottom of Figure 8 has 8 and 12 inter- and intramolecular HB, respectively. For this structure, the DMN guest is perfectly shielded against exposure to the solvent, much better than it was in the hypothetical 1:1 complex. The large negative ΔS for DMN:αCD_2 should proceed to the loss of degrees of freedom during its formation, as discussed in the previous section.

According to results of Tables 4 and 5, binding energies for the formation of 1:2 complexes are obviously more negative than for the formation of 1:1 ones. This fact agrees with the large negative enthalpy changes for the DMN:αCD_2 complex compared with the formation of the DMN:*β*CD one.

To try to answer the question of why MN only forms1:1 complexes with αCD[49] while DMN forms the DMN:αCD_2 ones, the contributions to $E_{binding}$(DMN−(host1+host2)) from both the ester groups and naphthalene ring were calculated separately. Thus, results for the structure depicted in Figure 8 show that the ester groups contribute with more than one-third of the total binding energy, with van der Waals as the most important interaction. This could suggest the possibility that the binding of MN to CD might occur at the ester substituent rather than at the apolar naphthalene group. This way of complexation should probably provide a better fit of the guest into the cavity. This fact has also been pointed out by several authors studying the complexation of other monosubstituted naphthalenes.[14,17,22] On the other hand, the presence of a second substituted ester group in DMN might favor the addition of a new αCD to the 1:1 DMN:αCD complex. Another reason for the better stabilization of the 1:2 complex could come from the possibility of the hydrogen-bonding of oxygens of the ester groups with the primary hydroxyl groups of αCD. Nevertheless, the structure depicted in Figure 8 does not show any of these HBs. However, small changes in the conformation of this structure might make the formation of such HBs possible.

Conclusions

Molecular mechanics calculations can reproduce the experimental evidence that 1:1 DMN:βCD and 1:2 DMN:αCD_2 complex formations are possible and the fact that the 1:2 DMNN:βCD_2 complex is not experimentally observed. The main reason for the formation of the 1:2 complex is that only part of the DMN can penetrate into the αCD cavity, stabilizing the system by shielding the guest with an additional αCD. The nonbonded van der Waals interactions are mainly responsible for the stability of both DMN:βCD and DMN:αCD_2 complexes. Nevertheless, hydrogen bonding between CDs and between carboxylic oxygens of ester groups and CD primary hydroxyl groups could also be the cause of stabilization of the 1:2 complex. Both complexations show a dependence of $\Delta H°$ and $\Delta S°$ on temperature with $\Delta C_p° < 0$, as do most of the processes of transfer of apolar guests from an aqueous medium to a hydrophobic environment. The DMN:αCD_2 complex formation is enthalpy-governed in the whole range of temperatures studied. However, the DMN:βCD complexation is enthalpy-driven at $T > 18$ °C and entropy-driven at $T < 18$ °C. Relative binding energies for both complexes seem to explain the relative changes of enthalpy upon formation. The 1:2 complex has considerably more negative binding energies than the 1:1 complex.

Acknowledgment. This research was supported by CICYT Grant PB97-0778. We express our thanks to M. L. Heijnen for assistance with the preparation of the manuscript.

References and Notes

(1) Bender, M. L.; Komiyama, M. *Cyclodextrins Chemistry*; Springer-Verlag: Berlin, 1978.
(2) Szejtli, J. *Cyclodextrins and Their Inclusion Complexes*; Akadémiai Kiadó: Budapest, 1982.
(3) Szejtli, J. *Cyclodextrins Technology*; Kluwer Academic Publisher: Dordrecht, 1988.
(4) Szejtli, J.; Osa, T. *Comprehensive Supramolecular Chemistry*; Elsevier: Oxford, 1996; Vol. 3, Cyclodextrins.
(5) VD'Souza, V. T.; Lipkowitz, K. B. *Chem. Rev.* **1998**, *98*, 8 (5), 1741.
(6) Bergeron, R. J.; Channing, M. A.; Gibeily, G. J.; Pillor, D. M. *J. Am. Chem. Soc.* **1977**, *20*, 5146.
(7) Ogino, H. *J. Am. Chem. Soc.* **1981**, *103*, 1303.
(8) Ogino, H.; Ohata, K. *Inorg. Chem.* **1984**, *23*, 3312.
(9) Manka, J. S.; Lawrence, D. S. *J. Am. Chem. Soc.* **1990**, *112*, 2440.
(10) Venkata, T.; Rao, S.; Lawrence, D. S. *J. Am. Chem. Soc.* **1990**, *112*, 3614.
(11) Isnin, R.; Kaifer, A. E. *J. Am. Chem. Soc.* **1991**, *113*, 8188.
(12) Wenz, G.; Keller, B. *Angew. Chem., Int. Ed. Engl.* **1992**, *31*, 197.
(13) Harada, A.; Li, J.; Kamachi, M. *Macromolecules* **1993**, *26*, 5698.
(14) Yorozu, T.; Hoshino, M.; Imamura, M.; Shizuka, H. *J. Phys. Chem.* **1982**, *86*, 4422.
(15) Nakajima, A. *Spectrochim. Acta* **1983**, *39A* (10), 913.
(16) Patonay, G.; Shapira, A.; Diamond, P.; Warner, I. M. *J. Phys. Chem.* **1986**, *90*, 1963.
(17) Agbaria, R. A.; Uzan, B.; Gill, D. *J. Phys. Chem.* **1989**, *93*, 3855.
(18) Takahashi, K. *J. Chem. Soc., Chem. Commun.* **1991**, 929.
(19) Flamigni, L. *J. Phys. Chem.* **1993**, *97*, 9566.
(20) Monti, S.; Köhler, G.; Grabner, G. *J. Phys. Chem.* **1993**, *97*, 13011.
(21) Schuette, J. M.; Warner, I. M. *Talanta* **1994**, *41* (5), 647.
(22) Fraiji, E. K., Jr.; Cregan, T. R.; Werner, T. C. *Appl. Spectrosc.* **1994**, *48* (1), 79.
(23) Nakamura, A.; Sato, S.; Hamasaki, K.; Ueno, A.; Toda, F. *J. Phys. Chem.* **1995**, *99*, 10952.
(24) Nelson, G.; Patonay, G.; Warner, I. M. *Appl. Spectrosc.* **1987**, *41* (7), 1235.
(25) Kobayashi, N.; Saito, R.; Hino, H.; Hino, Y.; Ueno, A.; Osa, T. *J. Chem. Soc., Perkin. Trans. 2* **1983**, 1031.
(26) Turro, N. J.; Okubo, T.; Weed, G. C. *Photochem. Photobiol.* **1982**, *35*, 325.
(27) Kano, K.; Takenoshita, I.; Ogawa, T. *Chem. Lett. Chem. Soc. Jpn.* **1982**, 231.
(28) Hamai, S. *Bull. Chem. Soc. Jpn.* **1982**, *55*, 2721.
(29) Hamai, S. *J. Phys. Chem.* **1989**, *93*, 6527.
(30) Catena, G. C.; Bright, F. V. *Anal. Chem.* **1989**, *61*, 905.
(31) Yorozu, T.; Hoshino, M.; Imamura, M. *J. Phys. Chem.* **1982**, *86*, 4426.
(32) Hashimoto, S.; Thomas, J. K. *J. Am. Chem. Soc.* **1985**, *107*, 4655.
(33) Nakajima, A. *Bull. Chem. Soc. Jpn.* **1984**, *57*, 1143.
(34) Street, K. W., Jr.; Acree, W. E., Jr. *Appl. Spectrosc.* **1988**, *43* (7), 1315.
(35) Muñoz de la Peña, A.; Ndou, T. T.; Zung, J. B.; Warner, I. M. *J. Phys. Chem.* **1991**, *95*, 3330.
(36) Muñoz de la Peña, A.; Ndou, T. T.; Zung, J. B.; Greene, K. L.; Live, D. H.; Warner, I. M. *J. Phys. Chem.* **1991**, *95*, 1572.
(37) Will, A. Y.; Muñoz de la Peña, A.; Ndou, T. T.; Warner, I. M. *Appl. Spectrosc.* **1993**, *47* (3), 277.
(38) Kusumoto, Y. *Chem Phys. Lett.* **1987**, *136*, 535.
(39) Edwards, H. E.; Thomas, J. K. *Carbohydr. Res.* **1978**, *65*, 173.
(40) Sherrod, M. J. In S*pectroscopic and Computational Studies of Supramolecular Systems*; Davies, J. E. D., Ed.; Kluwer Academic Publishers: Dordrecht, The Netherlands, 1992; p 187.
(41) VD'Souza, V. T.; Lipkowitz, K. B. *Chem. Rev.* **1998**, *98* (5), 1829.
(42) Madrid, J. M.; Pozuelo, J.; Mendicuti, F.; Mattice, W. L. *J. Colloid Interface Sci.* **1997**, *193*, 112.
(43) Madrid, J. M.; Mendicuti, F.; Mattice, W. L. *J. Phys. Chem. B* **1998**, *102*, 2037.
(44) Pozuelo, J.; Nakamura, A.; Mendicuti, F. *J. Inclusion Phenom. Macrocyclic Chem.* **1999**, *35* (3), 467.
(45) Madrid, J. M.; Villafruela, M.; Serrano, R.; Mendicuti, F. *J. Phys. Chem. B* **1999**, *103* (23), 4847.
(46) Pozuelo, J.; Mendicuti, F.; Mattice, W. L. *Macromolecules* **1997**, *30*, 3685.
(47) Pozuelo, J.; Mendicuti, F.; Mattice, W. L. *Polym. J.* **1998**, *30*, 479.
(48) Pozuelo, J.; Mendicuti, F.; Saiz, E. In *Proceedings of the 9th International Symposium on Cyclodextrins*; Labandeira, J. J., Vila, J. L., Eds.; Kluwer Academic Publishers: The Netherlands, 1999; p 567.
(49) Madrid, J. M.; Mendicuti, F. *Appl. Spectrosc.* **1997**, *51*, 1621.
(50) *Sybyl*, version 6.4; Tripos Associates: St. Louis, MO, 1997.
(51) Crark, M.; Cramer, R. C., III.; van Opdenbosch, N. *J. Comput. Chem.* **1989**, *10*, 982.
(52) MOPAC (AM1), included in the Sybyl 6.4 package.
(53) Brunel, Y.; Faucher, H.; Gagnaire, D.; Rasat, A. *Tetrahedron* **1975**, *31*, 1075.
(54) Press, W. H.; Flannery, B. P.; Teukolski, S. A.; Vetterling, W. T. *Numerical Recipes: The Art of Scientific Computing*; Cambridge University Press: Cambridge, 1988; p 312.
(55) Blanco, M. *J. Comput. Chem.* **1991**, *12*, 237.
(56) *MicroCal Origin*, version 4.0; MicroCal Software, Inc.: Northampton, MA, 1995.
(57) Harata, K. *Bull. Chem. Soc. Jpn.* **1979**, *52*, 1807.
(58) Inoue, Y.; Hakushi, T.; Liu, Y.; Tong, L.-H.; Shen, B.-J.; Jin, D.-S. *J. Am. Chem. Soc.* **1993**, *115*, 475.
(59) Guo, Q. X.; Zheng, X. Q.; Luo, S. H.; Liu, Y. C. *Chin. Chem. Lett.* **1996**, *7*, 357.
(60) Guo, Q.-X.; Zheng, X.-Q.; Ruan, X.-Q.; Luo, S. H.; Liu, Y. C. *J. Inclusion Phenom.* **1996**, *26*, 175.
(61) Godinez, L. A.; Schwartz, L.; Criss, C. M.; Kaifer, A. E. *J. Phys. Chem. B* **1997**, *101*, 3376.
(62) Park, H.-R.; Mayer, B.; Wolschann, P.; Köhler, G. *J. Phys. Chem. B* **1994**, *98*, 6158.
(63) Hamai, S. *J. Phys. Chem. B* **1995**, *99*, 12109.
(64) Hamai, S. *J. Phys. Chem. B* **1997**, *101*, 1707.
(65) Nakamura, A.; Sato, S.; Hamasaki, K.; Ueno, A.; Toda, F. *Phys. Chem.* **1995**, *99*, 10952.
(66) Rekharsky, M. V.; Inoue, Y. *Chem. Rev.* **1998**, *98* (5), 1875.
(67) Harrison, J. C.; Eftink, M. R. *Biopolymers* **1982**, *21*, 1153−1166.
(68) Rekharsky, M. V.; Schwarz, F. P.; Tewari, Y. B.; Goldberg, R. N.; Tanaka, M.; Yamashoji, Y. *J. Phys. Chem.* **1994**, *98*, 4098−4103.
(69) Hobza, P.; Zahradnik, R. *Intermolecular Complexes*; Elsevier: New York, 1988.